Academic Science Journal

Geochemical Characteristics of Clay Deposits, Bussaya Area, Southern Iraq

Ghassan F. Mezaal[1*], Kareem Khwedim[2], Imad K. Abdulzahra[1]

[1]Senior Chief Geologist, Iraq Geological Survey, Baghdad, Iraq

[2] Department of petroleum geology, College of Science, University of Diyala, Diyala, Iraq

* ghassangeo@gmail.com

Received: 24 July 2023 **Accepted: 18 September 2023**

DOI: https://dx.doi.org/10.24237/ASJ.02.04.785C

Abstract

This study concerned with the geochemical characteristics of clay deposits belong to Nfayil beds (Middle Miocene) in Al Muthana Governorate southern Iraq, as a new resource of clay raw material. Twenty three samples of clay deposits were analyzed by using X-Ray Fluorescence technique (XRF) for the major oxides; (SiO_2, Al_2O_3, Fe_2O_3, MgO, CaO, Na_2O, K_2O, TiO_2, and L.O.I), and trace elements; (V, Cr, Co, Ni, Cu, Zn, As, Sr, Pb, Ga, Rb, Ba, and Zr). The chemical results demonstrated due to the relation between Sr and Cu, that the depositional environment predominated by hot and arid paleoclimate conditions, while from the relation between Al_2O_3 with (Al_2O_3, CaO, Na_2O, and K_2O) reveals a low to relatively moderate chemical weathering. Whereas the ratio of Ni/Co reveals that the deposition was within hypoxic environment, while due to the ratio of Al_2O_3 / TiO_2 in which advocated by Ti- Zr relation which demonstrates that the intermediate igneous rocks as a provenance of the studied clays.

Keywords: Clay, geochemistry, Paleoclimate, Chemical weathering, raw materials.

الخصائص الجيوكيميائية لترسبات الاطيان، منطقة بصية، جنوب العراق

غسان فيصل مزعل[1] و كريم حسين خويدم وعماد كاظم عبد الزهرة[1]

[1]رئيس اقدم جيولوجيين – هيئة المسح الجيولوجي – بغداد – العراق

[2]قسم علوم جيولوجيا النفط والمعادن – كلية العلوم – جامعة ديالى

Academic Science Journal

الخلاصة

اهتمت هذه الدراسة بالخصائص الجيوكيميائية لترسبات الاطيان التابعة لطبقات النفايل (المايوسين المتوسط) في محافظة المثنى جنوب العراق كمصدر جديد للمواد الاولية الطينية, اذ تم تحليل ثلاثة وعشرون نموذجا من الطين بتنقية الاشعة السينية (XRF) للاكاسيد الرئيسية; (SiO_2, Al_2O_3, Fe_2O_3, MgO, CaO, Na_2O, K_2O, TiO_2, and L.O.I) والعناصر النزرة; (V, Cr, Co, Ni, Cu, Zn, As, Sr, Pb, Ga, Rb, Ba, and Zr), اذ اوضحت نتائج التحاليل الكيميائية من خلال العلاقة مابين السنتروتيوم و النحاس بأن البيئة الترسيبية التي ترسبت فيها الاطيان قد ساد فيها المناخ الحار الجاف, بينما اوضحت العلاقة بين اوكسيد الالمنيوم الى مجموع اكاسيد الالمنيوم مع الصوديوم والبوتاسيم والكالسيوم بأن التجوية الكيميائية كانت منخفضة الى متوسطة, في حين بينت العلاقة بين النيكل والكوبلت بأن الترسيب قد حدث في بيئة اختزالية, كذلك تبين من خلال نسبة اوكسيد الالمنيوم الى اوكسيد التيتانيوم ان اصل الاطيان هو صخور نارية متوسطة علما ان هذا الاستنتاج قد دعم بمخطط للعلاقة بين التيتانيوم والزركون.

الكلمات المفتاحية: الطين, جيوكيمياء, المناخ القديم, تجوية كيميائية, مواد خام .

Introduction

According to [1], clay is a form of naturally occurring, fine-grained soil that is composed of particular kinds of hydrous aluminum, magnesium, and iron silicates, some of which may also contain sodium, calcium, potassium, and other ions. Clay deposits considered as a raw material for many industrial such as constructions (Portland cement, ceramic, brick...etc.), paper making, house stuff, in addition to the creation of products with high added value like nano-composites, cosmetics, and pharmaceuticals, geochemical data is extremely important as a source rock indicator, clay deposits within the upper member of Nfayil beds (middle Miocene), which introduced by [2] due to the absence of the evaporate beds, it is important to find a new resource of raw materials due to the usage of the recent clay deposits of the agricultural soils for industrial purposes which caused lack of industrial clays, the main aim of this study is to determine the geochemical characteristics because they are crucial for the demands of industry.

Study area and lithostratigraphy

Study area is located within Al-Muthana governorate, north east of Bussayah Township, where the clay deposits of Nfayil Beds (middle Miocene). It was located within (long. 46°18' - 46°19') and (lat. 30°28' - 30°29') coordinates (Table 1), which included within southern desert of Iraq,

Academic Science Journal

Figure (1 and 2), , according to [3]; Ghar Formation (Early Miocene), exposed west and southwest of the study area, with conformable upper contact with the claystone of the Nfayil beds, the clay deposits of the study interbedded within the upper unit of the Nfayil beds which consist of sand, sandstone, and calcareous sandstone with restricted lenses of marl and sandy limestone [4], Figure (3).

Table 1: Study area coordinates

Easting	Northing
46°18'47"	30°28'48"
46°18'49"	30°29'36"
46°19'03"	30°28'49"
46°19'18"	30°28'58"
46°19'19"	30°29'37"

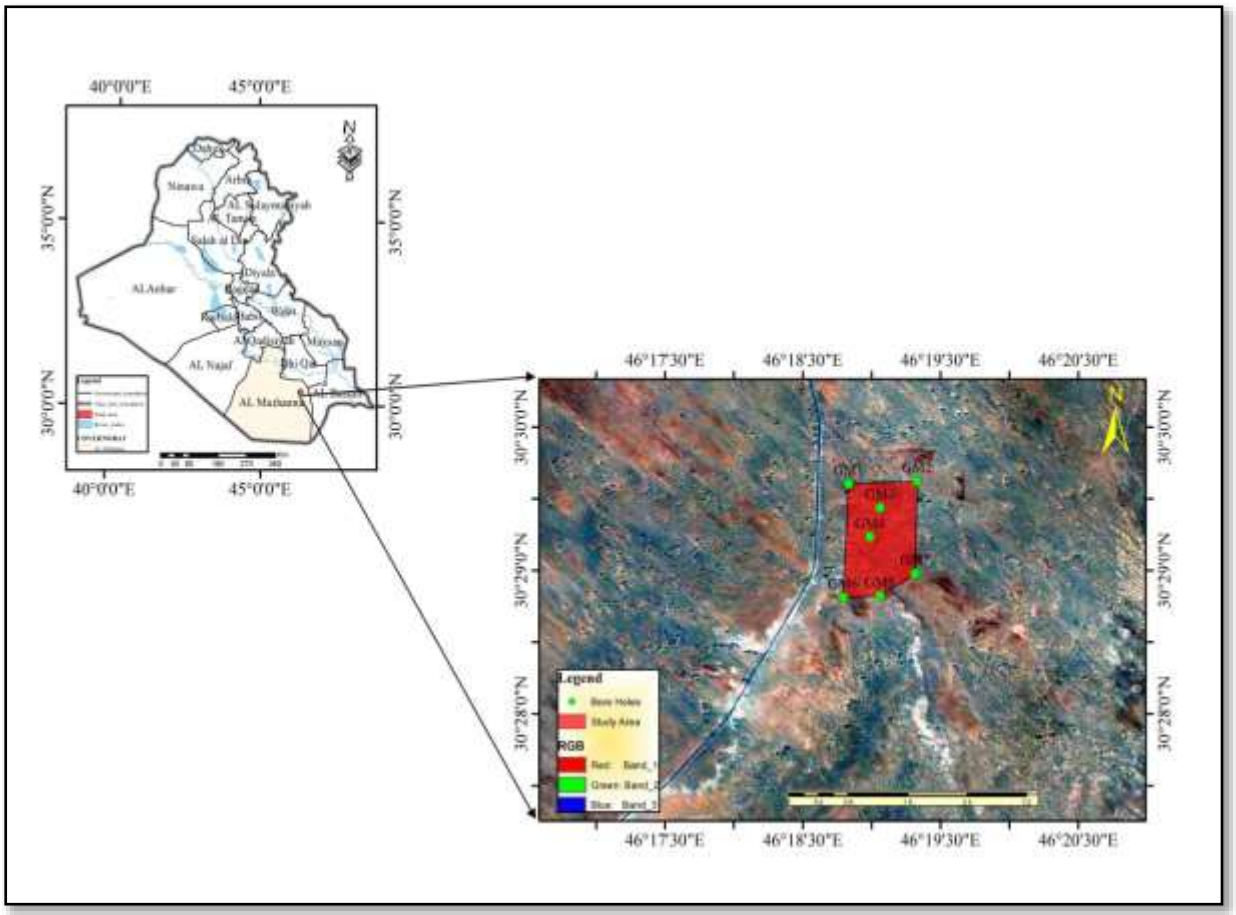

Figure 1: Location map of the study area

Academic Science Journal

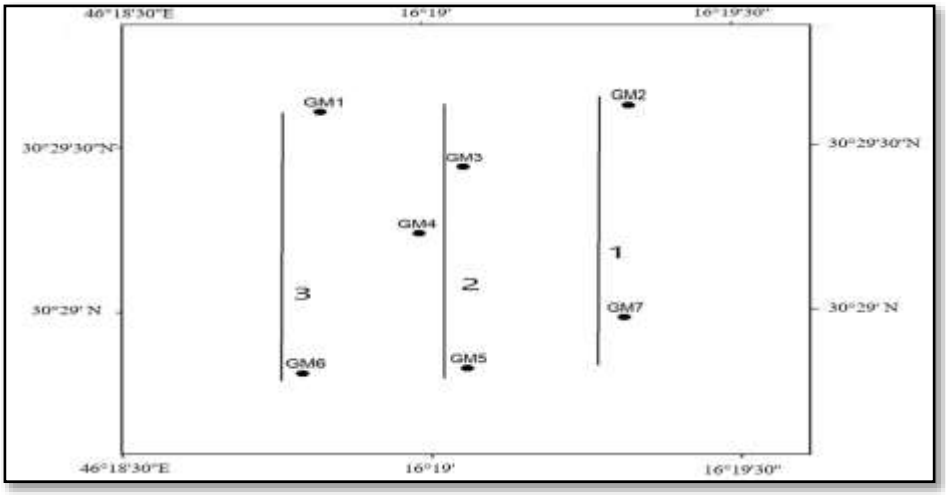

Figure 2: Boreholes location and cross sections distributions

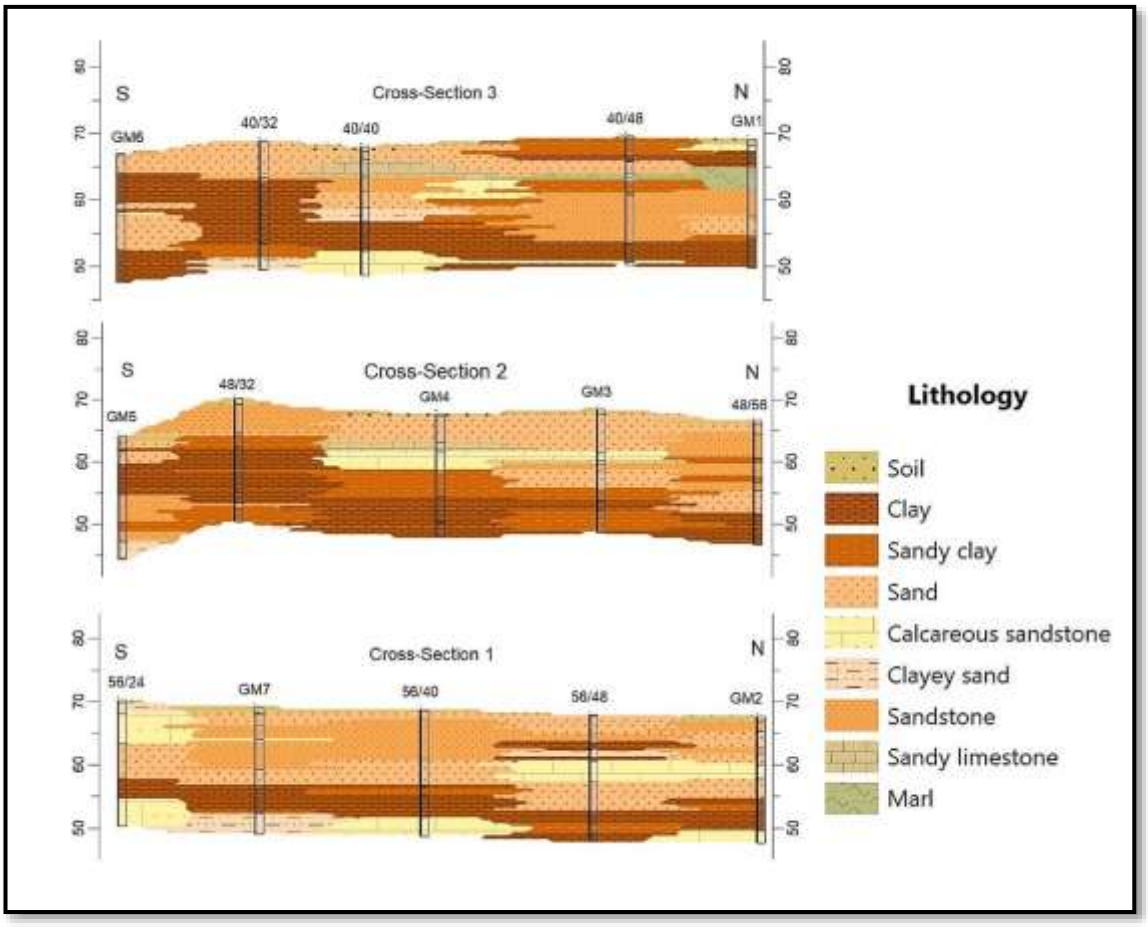

Figure 3: Cross sections show the clay distribution throughout the study area

Materials and Methods

Seven of the fifteen boreholes (with an average spacing of 400 x 400 m) were chosen for sampling, and clay samples were taken at varied depths across the boreholes. Twenty-three samples were taken from the boreholes dug by the Iraq Geological Survey at a depth of (20 m), (Table, 2).

Table 2: boreholes locations and clay depths

Borehole NO.	Location		Depth intervals of clay (M)
	Longitude	Latitude	
GM1	46°18'49"	30°29'36"	2 – 4.3 / 15.7 - 20
GM2	46°19'19"	30°29'37"	13 – 14 / 14.8 – 18
GM3	46°19'3"	30°29'26"	14.6 – 16.4
GM4	46°18'59"	30°29'14"	13.3 – 20
GM5	46°19'3"	30°28'49"	2.2 – 2.6 / 4.7 – 9.7
GM6	46°18'47"	30°28'48"	3 – 7.7 / 15 – 20
GM7	46°19'18"	30°28'58"	12.4 – 16.4

Samples of clay deposits were analyzed by using XRF technique for the major oxides; (SiO_2, Al_2O_3, Fe_2O_3, MgO, CaO, Na_2O, K_2O, TiO_2, and L.O.I), and trace elements; (V, Cr, Co, Ni, Cu, Zn, As, Sr, Pb, Ga, Rb, Ba, and Zr).

Results and Discussions

The percentage and concentrations of the major oxides and trace elements are shown in Table (3 and 5), while the chemical composition of the studied sample are described as follow:

Major Oxides

Silica (SiO_2)

With a range of (31.97 - 45.78%) and an average of (39.17%), silica is the most prevalent oxide (Table, 3), the majority of the reason for the significantly high percentage in comparison to other oxides is due to the clay mineral's crystal structure, which contains silica oxides and contains quartz, as expressed by the positive correlation coefficient with the clay forming minerals

(aluminum, iron, and potassium oxides), and inversely correlated with CaO and MgO (Table, 4), which mean that there is no association [5].

Aluminum oxide (Al_2O_3)

With an average of 9.95%, aluminum oxide ranged from (7.938 - 12.16%) (Table, 3), this oxide comes from clay minerals, which contain aluminum oxide as a structural component, the quantity of clay minerals affects how aluminum is distributed [6], which are positively correlated with potassium and iron oxides (Table, 4), and entering the chemical composition of illite.

Iron Oxide (Fe_2O_3)

Table (3) shows that the average percentage of iron oxide in the examined samples was 6.21%, with a range of 4.512 to 6.94%, the positive correlation between Fe_2O_3, SiO_2, and Al_2O_3 is shown in (Table, 4), and there is also a substantial positive correlation between it and titanium oxide, indicating that it has been incorporated into the internal structure of illite in addition that they come from a similar sources.

Magnesium Oxide (MgO)

With an average value of 5.9%, magnesium oxide percentage ranged from (4.75 - 8.79%) (Table, 3), this comparatively high MgO content is due to the oxide's presence in clay minerals like palygoreskite and chlorite, as well as dolomite, and (Table, 4) demonstrates a strong positive association between MgO and CaO, indicating that they originated from the same source and were probably carried out by carbonate-bearing fluids.

Table 3: Major oxides concentrations

Sample NO.	SiO_2 %	Al_2O_3 %	Fe_2O_3 %	MgO %	CaO %	Na_2O %	K_2O %	TiO_2 %	L.O.I %
GM1-A	36.19	8.676	6.38	5.215	8.68	11.62	1.222	0.9157	13.25
GM1-B	36.88	10.37	6.366	5.11	5.47	10.43	2.218	0.8562	14.95
GM1-C	38.27	9.214	6.342	5.283	7.98	8.117	1.182	0.9089	16.12

GM2-A	37.82	9.051	5.56	5.094	9.19	8.556	2.126	0.9493	16.07
GM2-B	38.06	9.202	5.593	5.189	9.26	7.891	2.138	0.9527	13.06
GM2-C	38.34	9.202	6.394	5.078	8.51	8.906	2.115	0.929	14.79
GM3-A	39.47	9.719	6.682	5.3	10.86	6.004	1.262	0.9774	13.25
GM3-B	38.98	9.379	6.227	5.114	11.7	6.978	2.157	0.8591	13.88
GM4-A	45.78	11.01	5.528	6.69	8.281	4.401	2.15	0.8428	11.85
GM4-B	39.07	9.34	6.377	5.087	11.99	4.201	1.122	1.003	17.94
GM4-C	39.58	11.638	6.485	5.32	10.07	4.977	1.184	0.9682	17.03
GM4-D	38.83	10.359	6.455	5.207	12.96	5.925	1.171	0.9505	15.33
GM5-A	40.48	9.285	5.871	4.752	11.48	4.396	1.111	0.991	18.21
GM5-B	43.57	12.16	6.944	6.108	9.973	3.125	2.484	0.8358	12.76
GM5-C	41.34	10.975	5.832	6.1	10.72	4.189	2.127	0.8538	14.51
GM5-D	38.3	10.305	6.437	5.343	12.34	3.945	2.179	0.9137	18.29
GM5-E	43.81	10.805	6.881	6.32	11.11	2.009	2.32	0.9747	14.78
GM5-F	41.04	11.583	6.579	7.169	12.89	0.949	2.263	0.8976	16.84
GM6-A	31.97	7.938	4.512	8.798	14.79	5.232	1.614	0.5984	20.87
GM6-B	38.44	9.411	6.472	7.208	18.13	5.031	1.507	0.9313	9.9
GM7-A	39.11	10.901	6.178	7.038	13.48	4.267	1.341	0.9315	12.9
GM7-B	38.38	9.381	6.404	6.36	14.09	5.98	1.212	0.8991	14.21
GM7-C	37.32	9.054	6.512	6.939	15.99	6.233	1.153	0.9127	12.79
Range	31.97 - 45.78	7.93 – 12.16	4.51 – 6.88	4.75 – 8.79	5.46 – 15.99	0.94 – 11.62	1.11 – 2.48	0.59 – 1.003	9.9 – 20.87
Av.	39.17	9.95	6.21	5.9	11.3	5.79	1.71	0.9	14.94

Calcium Oxide (CaO)

With an average value of (11.3%), calcium oxide varied from (5.46 to 18.13%) (Table 3), carbonate-bearing water, the weathering of pyroxene and amphibole minerals within the source areas, and the presence of dolomite in the clay all contribute to the clay's relatively high percentage of calcium oxide.

Sodium Oxide (Na_2O)

Sodium oxide ranged from (0.94 – 11.62%) with average value of (5.79%) (Table, 3), the predominant oxide in feldspar is Na_2O in which considered as a one of assumed sources, and also occurs as Na+ adsorbed on clay particles or in fluids due to its high mobility in solutions [7], (Table, 5) shows that (Na_2O) does not correlate with other oxides.

Potassium Oxide (K_2O)

Potassium oxide ranged from (1.11 – 2.48%) with average value of (1.71%) (Table, 3), the source of K_2O is the presence of K^+ in clay minerals such illite, as well as orthoclase and microcline, and mica (muscovite) minerals through weathering these rocks [6-7], due to the inclusion of both elements in the crystal structure of the illite clay mineral, K_2O demonstrates a positive connection with SiO_2 and Al_2O_3, Table (4).

Table 4: Correlation Coefficient of major oxides

	SiO2	Al2O3	Fe2O3	MgO	CaO	Na2O	K2O	TiO2	L.O.I
SiO2	1								
Al2O3	0.737	1							
Fe2O3	0.396	0.464	1						
MgO	-0.117	0.023	-0.330	1					
CaO	-0.207	-0.170	0.000	0.608	1				
Na2O	-0.550	-0.575	-0.150	-0.447	-0.472	1			
K2O	0.369	0.391	-0.038	0.050	-0.348	-0.162	1		
TiO2	0.344	0.149	0.593	-0.649	-0.097	0.001	-0.274	1	
L.O.I	-0.369	-0.182	-0.361	-0.030	-0.050	-0.159	-0.104	-0.233	1

Titanium Oxide (TiO_2)

The average value of titanium oxide was (0.906%), with a range of (0.59 - 1.003 %) (Table, 3), The difference in titanium oxide concentration is determined by the capacity to replace iron and aluminum instead, as well as the cation exchange capacity, which rises as clay volume and clay minerals expand [8], there is a positive correlation with SiO_2 & Al_2O_3, significantly with Fe_2O_3, (Table, 4).

Loss on Ignition (L.O.I)

The LOI is a result of sample burning, which results in the release of carbon dioxide (CO_2) from carbonate minerals and the loss of water content from clay minerals, its percentage ranged from (9.9 – 20.87%) with average value of (14.94%) (Table, 3), a negative correlation coefficient between L.O.I. and the other main oxides in the samples is seen in (Table, 4).

Trace Elements

Vanadium (V)

Vanadium's average concentration was (222.65) ppm, with a range of (128 – 416) ppm (Table, 5). V is adsorbed on the surfaces of clay minerals, inside the structure of minerals, or in combination with iron oxides, [9], (Table, 6) shows a positive correlation between V and (SiO_2, Al_2O_3, Fe_2O_3, K_2O).

(Cr, Co, Ni, and Cu)

They have average value of (529, 20, 244, and 45) ppm respectively (Table, 5), and shows a positive correlation coefficient (Table, 7), moreover; positively correlated with iron and titanium oxides, [10] attributed the explanation for the Ni concentrations to the existence of iron impurities in muds, copper has a positive correlation with Silica, aluminum, oxides, and significantly with iron and titanium oxide (Table, 6), this demonstrates its interaction with feldspar and clay minerals, as well as its adsorption on the illite mineral or adsorbed on iron oxides [11].

(Zn, Sr, Pb, and Ba)

They have average value of (106, 442, 12.43, and 247.8) ppm respectively (Table 4), and shows a positive correlation coefficient (Table, 7), Zn is adsorbed on the surfaces of clay minerals (kaolinite and illite) [12], It demonstrates the positive correlation between Zn and the clay-forming minerals SiO_2, Al_2O_3, Fe_2O_3, and K_2O (Table, 6), lead is a naturally occurring element of the earth's crust that can occur naturally and heterogeneously in the soil due to the weathering, erosion, and deposition of crustal materials as well as the deposition of lead released into the

earth's atmosphere by volcanic activity [13]; [14], while barium is mostly found in rock-forming minerals such as K-feldspar, mica, apatite, and calcite, as well as in soil components, [15].

(As, Ga, Rb, and Zr)

They have average value of (14.78, 14.6, 50.78, 176.47) ppm respectively (Table, 5), also shows a positive correlation coefficient (Table, 7), positively correlated with clay forming minerals (Table, 6), inversely correlated with (Cr, Co, Ni, and Cu), rubidium may be adsorbed on the surface of clay minerals, particularly illite, when potassium is substituted for rubidium [16].

The trace elements of the studied clays had been separated into three groups based on their abundance through comparison with the typical shale's trace elements [17]. According to the proposed boundaries of [18], the trace elements with twice as much (X2) existence are considered to be "enriched," while those with half as much existence or less are considered to be "depleted." Elements that fall in the middle of the two ranges are considered to have a "normal" existence.

The comparison in (Table, 8) shows that the normal state is represented by Co, Cu, and Zn, but there is enrichment with V, Cr, Ni, and Sr and depletion with Pb and Zr.

Table 5: Trace elements concentrations (ppm)

Sample NO.	V	Cr	Co	Ni	Cu	Zn	As	Sr	Pb	Ga	Rb	Ba	Zr
GM1-A	240	541	31	258	51	116	11	595	14	15	47	261	165
GM1-B	285	141	8	138	47	107	35	142	12	20	74	179	204
GM1-C	147	634	21	271	46	111	11	529	13	14	47	263	176
GM2-A	196	504	26	266	48	113	12	536	12	13	47	225	178
GM2-B	200	485	24	273	49	112	11	536	12	14	48	259	165
GM2-C	234	663	17	269	46	98	11	494	12	14	45	268	173
GM3-A	210	651	14	285	49	111	13	512	13	14	50	269	182
GM3-B	128	530	21	277	45	99	11	478	12	15	47	260	169
GM4-A	251	374	9	162	35	92	28	146	11	16	66	229	247
GM4-B	267	840	21	253	43	98	11	496	11	14	45	267	183
GM4-C	176	641	33	272	45	104	12	489	12	15	48	270	165
GM4-D	239	647	24	267	46	107	10	494	13	14	47	255	178
GM5-A	160	624	20	242	41	106	8	588	13	12	43	280	187
GM5-B	416	178	8	155	39	115	44	119	13	20	78	220	218
GM5-C	228	435	9	240	44	98	9	678	12	14	42	240	161
GM5-D	223	585	23	278	45	103	11	505	13	14	48	262	174

Academic Science Journal

GM5-E	190	440	21	286	53	121	13	536	13	15	53	275	175
GM5-F	216	562	14	278	48	111	13	491	14	15	50	261	181
GM6-A	223	137	9	113	28	83	20	119	7	11	53	133	127
GM6-B	230	697	24	275	46	103	12	469	15	13	48	254	170
GM7-A	241	753	34	259	45	112	11	186	15	15	46	270	155
GM7-B	183	682	24	274	46	106	12	490	13	15	48	255	156
GM7-C	238	419	16	219	50	110	11	536	11	14	48	246	170
Range	128 – 416	137 – 840	8 – 34	113 – 285	28 – 53	83 – 112	8 – 44	119 – 678	7 – 15	13 – 20	43 – 74	133 – 280	127 – 247
Av.	222.65	529	20	244	45	106	15	441.9	12	14.6	51	248	176.48

Table 6: Correlation coefficient between major oxides and trace elements

	SiO2	**Al2O3**	**Fe2O3**	**MgO**	**CaO**	**Na2O**	**K2O**	**TiO2**	**L.O.I**
V	0.204	0.402	0.214	0.173	-0.087	-0.117	0.290	-0.212	-0.240
Cr	0.040	-0.104	0.323	-0.326	0.270	-0.076	-0.548	0.713	-0.049
Co	-0.195	-0.134	0.175	-0.272	0.163	0.181	-0.464	0.546	-0.051
Ni	0.106	-0.030	0.446	-0.411	0.163	-0.048	-0.221	0.746	-0.127
Cu	0.070	0.038	0.644	-0.451	-0.102	0.244	-0.044	0.722	-0.365
Zn	0.244	0.251	0.628	-0.318	-0.170	0.061	0.015	0.587	-0.341
As	0.258	0.410	0.048	0.168	-0.350	-0.028	0.471	-0.448	-0.169
Sr	-0.020	-0.243	0.239	-0.457	0.093	0.089	-0.260	0.597	0.044
Pb	0.347	0.367	0.669	-0.266	0.054	-0.070	-0.065	0.630	-0.505
Ga	0.403	0.615	0.493	-0.170	-0.484	0.067	0.428	-0.018	-0.374
Rb	0.304	0.438	0.119	0.138	-0.372	-0.025	0.485	-0.372	-0.217
Ba	0.413	0.179	0.593	-0.485	0.054	-0.164	-0.268	0.858	-0.250
Zr	0.709	0.485	0.259	-0.267	-0.469	-0.100	0.345	0.178	-0.329

Table 7: Correlation coefficient of trace elements

	V	**Cr**	**Co**	**Ni**	**Cu**	**Zn**	**As**	**Sr**	**Pb**	**Ga**	**Rb**	**Ba**	**Zr**
V	1												
Cr	-0.425	1											
Co	-0.417	0.676	1										
Ni	-0.564	0.815	0.666	1									
Cu	-0.236	0.385	0.446	0.709	1								
Zn	0.067	0.131	0.370	0.434	0.773	1							
As	0.753	-0.733	-0.598	-0.776	-0.406	-0.030	1						
Sr	-0.560	0.556	0.383	0.784	0.625	0.288	-0.795	1					
Pb	-0.002	0.511	0.474	0.604	0.619	0.673	-0.186	0.288	1				
Ga	0.618	-0.417	-0.287	-0.351	0.122	0.330	0.777	-0.483	0.235	1			
Rb	0.696	-0.725	-0.567	-0.719	-0.296	0.056	0.982	-0.766	-0.127	0.812	1		
Ba	-0.358	0.804	0.573	0.861	0.621	0.470	-0.591	0.657	0.677	-0.137	-0.534	1	
Zr	0.444	-0.222	-0.412	-0.295	-0.090	0.104	0.611	-0.326	0.137	0.602	0.658	0.036	1

Table 8: Trace elements averages of (BCD) in comparison with average shale of [17]

Elements	Av. Shale (ppm)	(BCD) ppm
V	130	222.65
Cr	90	529
Co	19	20
Ni	68	244
Cu	45	45
Zn	95	106
Sr	160	441.9
Pb	20	12
Zr	300	176.48

*(BCD): Bussaya Clay Deposits

Geochemical Ratios

Numerous geological applications can benefit from the use of geochemical ratios; for example, it is feasible to infer the source rocks of the clays under study and their associated weathering conditions by analyzing the distribution of major oxides and trace elements. Additionally, it may be possible to determine the paleoenvironment.

Provenance

According to [19], geochemical signatures can be used as an additional tool to identify the origin of sedimentary rocks, in order to identify the source rocks for sedimentary rocks, the ratio of Al_2O_3 / TiO_2 is utilized as a suitable geochemical indicator [20], In mafic, intermediate, and felsic igneous rocks, the ratios of Al_2O_3 / TiO_2 range from 3 - 8, 8 - 21, and 21 - 70 respectively [21], and according to the chemical analyses (Table, 9), Al_2O_3 / TiO_2 ratio ranged from (9.5 – 14.5) with average of (11.1) indicating that intermediate igneous rocks were the provenance of the studied clays, this conclusion is also supported by a bivariate TiO_2 - Zr plot [21], that shows the examined clays were derived from intermediate igneous rocks, Figure (4).

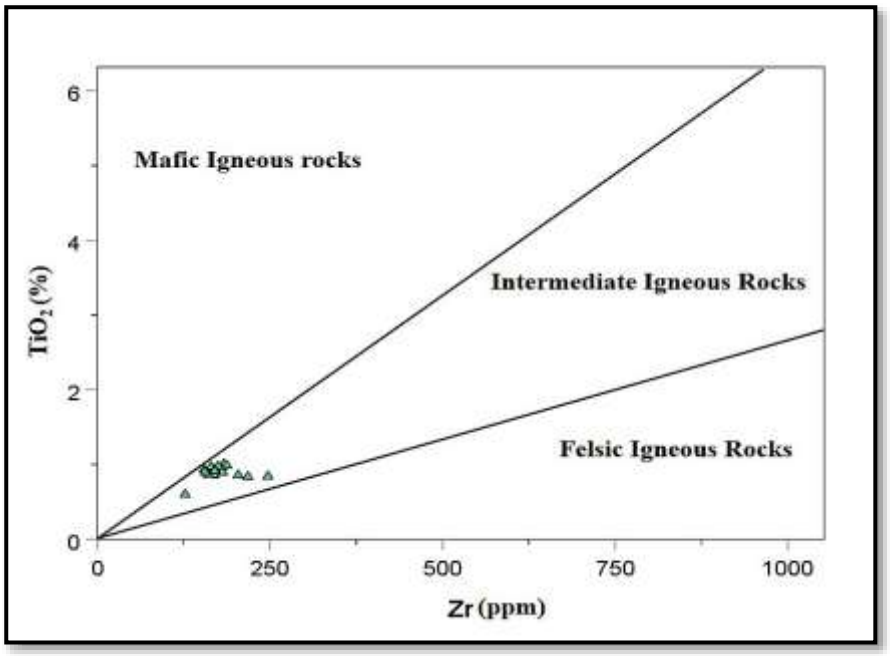

Figure 4: Bivariate plot of TiO_2 and Zr [21]

Chemical weathering

Chemical Index of Alteration (CIA), a widely used indicator of weathering and alteration for the source area, which was suggested by [22], and calculated by the following formula:

$$CIA = [Al_2O_3/ (Al_2O_3 + CaO^* + Na_2O + K_2O)] \times 100 \quad \ldots\ldots\ldots\ldots\ldots \quad (1)$$

Where (CaO*) simply denotes the (Ca) that is only included in the silicate fraction [23], the formula shown below can be used to adjust CaO*, according to [24].

$$CaO^* = 0.35 * 2\ (Na_2O\ \%)\ /62 \quad \ldots\ldots\ldots\ldots\ldots \quad (2)$$

Low chemical weathering is defined as less than 60; moderate chemical weathering is defined as 60–80; and strong chemical weathering is defined as more than 80 [25], the CIA values ranged from 40.1 – 78.2 % (Table, 9), which indicates low to moderate chemical weathering, clay samples were plotted on the CIA versus Al_2O_3 diagram [26], Figure (5).

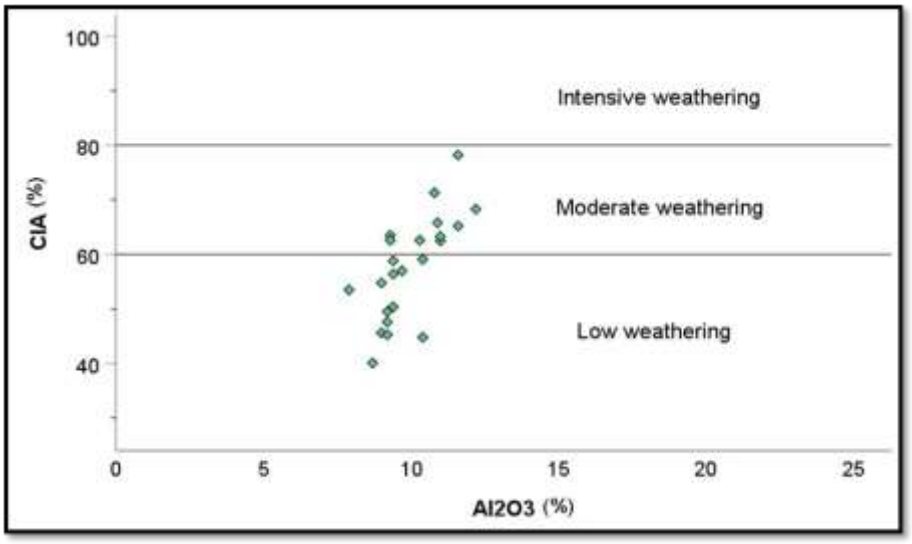

Figure 5: CIA vs Al_2O_3 diagram for the chemical weathering of the studied samples after [26]

Table 9: Geochemical ratios

Sample No.	Ni / Co	Sr / Cu	CIA %	Al_2O_3 / TiO_2
Range	7.62 – 26.67	3.02 – 15.41	40.1 – 78.2	9.31 – 14.54
Av.	13.88	9.64	57.6	11.06

Paleoredox

According to [27] and [28], the Ni/Co ratios of these elements can be utilized to determine paleoredox conditions. According to [29], these components have been significantly increased in a reductive environment.

Oxidizing conditions are indicated by Ni/Co values below 5 and hypoxia precipitating cases over 5, respectively, according to [30]; [29]. A hypoxic precipitating environment is indicated by the ratio, which in the examined clays ranged from 7.62 to 26.67 with an average of 13.88 (Table, 9).

Paleoclimate

The Sr/Cu ratio is a helpful indicator of paleoclimate; when it lies between (1.3 and 5.0), it indicates a warm, humid environment, whereas values higher than (5.0) indicate a hot and arid

environment [31]. The ratio ranges from 3.02 to 15.41, with an average of 9.64, as shown in (Table, 9), indicating a hot and arid climate.

Conclusion

According to statistics, the major oxides show diverse correlation coefficients, which reflects various sediment constituents and their origin and sedimentary conditions, low to moderate chemical weathering recognize the clays due to the influence of hot to arid paleoclimatic conditions, with hypoxic precipitating environment , and they are most probably derived from intermediate source rocks, also there is enrichment with (V, Cr, Ni, and Sr) and depletion with (Pb and Zr), while the normal existence is represented by (Co, Cu, and Zn).

References

1. W. W. Olive, A. F. Chleborad, C. W. Frahme, Shlocker, Julius, R. R. Schneider, R. L. Schuster, Swelling Clays Map of the Conterminous United States, (1989)
2. V. K. Sissakian, A. I. Mahdi, R. M. Amin, B. M. Salman: The Nfayil Formation: A new litho-stratigraphic unit in the Western Desert of Iraq, Iraqi Geological Journal, 30(1), 61–65 (1997)
3. M. T. Zaini, W. P. Beshir, K. N. AL-Kubaisi, F. Z. Kadhem, B. A. AL-Samarraie, H. A. Mousa, A. Al-Obaidy, Report on geological mapping scale 1:25 000 of south AL-NASIRIYA area (second stage). GEOSURV, int. rep. no. 3523 (2014)
4. S. T. Ahmed, H. Dh. Abdulwhab, M. F. Karim, Investigation of stratigraphic clay and sand in Al Muthana Governorate, category C2, Iraq Geosurv, Internal report (2022)
5. C. Micó, L. Recatalá, M. Peris, J. Sánchez, Assessing heavy metal sources in agricultural soils of an European Mediterranean area by multivariate analysis, Chemosphere, 65(5), 863-872 (2006)
6. F. H. Tobia, S. S. Shangola, Geochemistry of sandstones from Beduh formation in northern thrust zone, Kurdistan region, northern Iraq: provenance and tectonic sett, The Iraqi Geological Journal, 15-39 (2019)

7. N. S. Heier, G. K. Billings, Lithium. In: Wedepohl, K.H. (Ed.), Handbook of Geochemistry, Springer, Berlin, 3- G–13-H-1 (1978).
8. M. A. Al-Jobouri, Geochemistry of Colored Argillites of Fat'ha Formation (Middle Miocene) and their Industrial Significance at Selected Areas in Northern Iraq, M.Sc. thesis, College of Science, Mosul University, (in Arabic) (2005)
9. S. Landergren Vanadium; In: Handbook of Geochemistry (ed.) Wedepohl K W, (Springer-Verlag, Berlin, 1978), 23.D.1–23.D.10 1978
10. Y. M. Zainal, Mineralogy, Geochemistry and Origin of some Tertiary bentonite in Iraq. Ph.D. thesis, Sheffield, University of Sheffield. U.K. (1977)
11. S. Mackenzie, R. L. Patience, J. R. Maxwell, M. Vandenbroucke, and B. Durand, Molecular parameters of maturation in the Toarcian shales, Paris Basin, France. Changes in the configurations of acyclic isoprenoid alkanes, steranes and triterpanes. Geochimica et Cosmochimica Acta, 44(11), 1709-1721 (1980)
12. H. Farrah, W. F. Pickering, Extraction of heavy metals ions sorbed on clays, Water, Air and Soil Pollution, 9, 491-498 (1977)
13. E. Callender, Heavy metals in the environment-historical trends. Treatise on Geochemistry, 9, 67–105 (2003)
14. D. O'Connor, D. Houm, Y. J. Zhang, Y. S. Song, L. Tian, Lead-based paint remains a major public health concern: A critical review of global production, trade, use, exposure, health risk, and implications, Environmental International, 121, (2018)
15. P. Madejon, (2012). Barium. In: Alloway, B.J. (Ed.), Heavy Metals in Soils. Trace Metals and Metalloids in Soils and Their Bioavailability, Springer Science + Business Media, the Netherlands, Dordrecht, 507- 514 (2012)
16. V. M. Goldshmidt, Geochemistry, Oxford university press, London, 730p (1970)
17. K.K. Turekian, Wedepohl, K. H.: Distrybution of the elements in some major units of the Earth's crust, (Geological Society of America, bulletin 72, 1961), 175-192
18. J. S. Tooms, C. P. Summerhayes, D. S. Cronan, , Geochemistry of marine phosphate and manganese deposits, Ann. Rev. Oceanog. Mar. Biol, 7, 247-266 (1969)

19. J. Madhavaraju, S. Ramasamy, Petrography and geochemistry of Late Maastrichtian-Early Paleocene sediments of Tiruchirapalli Cretaceous, Tamil Nadu – Paleoweathering and provenance implications. – J. Geol. Soc. India. 59: 133 –142 (2002)
20. P. O. D. Andersson, R. H. Worden, D. M. Hodgson, S. Flint, Provenance evolution and chemostratigraphy of a Palaeozoic submarine fan-complex: Tanqua Karoo Basin, South Africa. – Mar. Petrol. Geol. 21, 555 – 577 (2004)
21. K. Hayashi, H. Fujisawa, H. Holland, H. Ohmoto, Geochemistry of 1.9 Ga sedimentary rocks from northeastern Labrador, Canada. Geochim. Cosmochim. Acta., 61, 4115 – 4137 (1997)
22. H. W. Nesbitt, G. M. Young, Early Proterozoic climates and plate motions inferred from major element chemistry of lutites, Nature Journal, 299, 715-717 (1982)
23. C. Baiyegunhi, K. Liu, O. Gwavava Geochemistry of sandstones and shales from the Ecca Group, Karoo Super group, in the Eastern Cape Province of South Africa: Implications for provenance, weathering, and tectonic setting. Open Geosciences, 9, (1), 340-360 (2017)
24. M. Honda, H. Shimizu, Geochemical, mineralogical and sediment-logical studies on the Taklimakan Desert sands. Sedimentology, 45, (6), 1125-1143 (1998)
25. M. Singh, M. Sharma, H. J. Tobschall, Weathering of the Ganga alluvial plain, northern India: implications from fluvial geochemistry of Gomati River, Applied Geochemistry, 20, 1-21 (2005)
26. R. A. Obasi, H. Y. Madukwe, Use of geochemistry to study the provenance, tectonic setting, source-area weathering and maturity of Igarra marble, Southwest, Nigeria. American Journal of Engineering Research, 5, (6), 90-99 (2016)
27. M. A. Ramos-Vázquez, J. S. Armstrong-Altrin, L. Rosales-Hoz, M. L. Machain-Castillo, and A. Carranza-Edwards. Geochemistry of deep-sea sediments in two cores retrieved at the mouth of the Coatzacoalcos River delta, western Gulf of Mexico, Mexico. Arabian Journal of Geosciences, 10(6), 1-19(2017)

28. Anaya-Gregorio, Abigail, Textural and geochemical characteristics of late Pleistocene to Holocene fine-grained deep-sea sediment cores (GM6 and GM7), recovered from southwestern Gulf of Mexico, Journal of Palaeogeography, 7.1, 1-19(2018)
29. S. Faraj, S. Pachidi, and K. Sayegh. Working and organizing in the age of the learning algorithm. Information and Organization, 28(1), 62-70 (2018)
30. D. M. McKirdy, P. A. Hall, Paleoredox status and thermal alteration of the lower Cambrian (series 2) Emu Bay shale Lagerstatte, South Australia. Australian J Earth Sci, 58: p 259 – 272 (2011)
31. B. M. S. Yandoka, H. A. Wan, M. B. Abubakar, M. H. Hakimi, A. K. Adegoke, Geochemical characterization of Early Cretaceous lacustrine sediments of Bima Formation, Yola Sub-basin, Northern Benue Trough, NE Nigeria: Organic matter input, preservation, paleoenvironment and palaeoclimatic conditions, Mar. Petrol. Geol. p 61, 82. (2015)